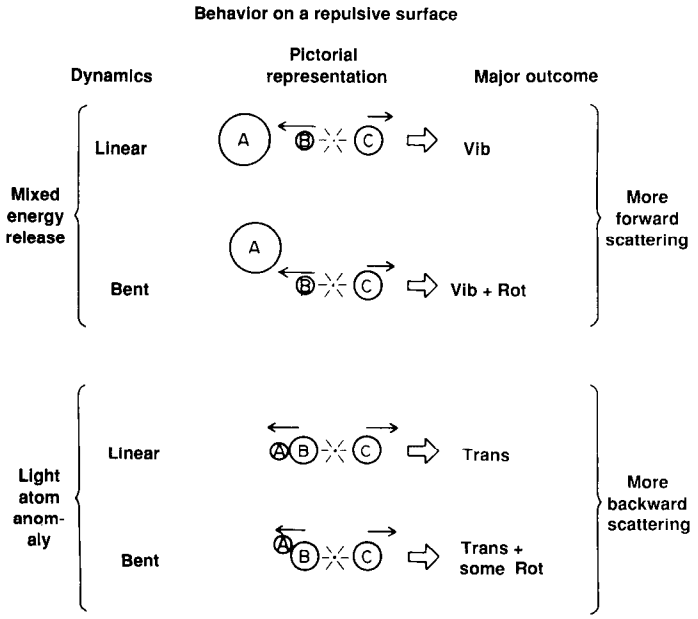


**Fig. 9.** Pictorial representation of contrasting types of reaction dynamics on a repulsive energy surface. "Mixed energy release," is commonly observed. "The light-atom anomaly" is observed if the attacking atom is very light. [Courtesy of *Accounts of Chemical Research* (*58*)]

chosen mass combination. The **L+HH** mass combination is in fact anomalous in fulfilling the initial expectation that repulsive energy release $\mathscr{R}_\perp$ (energy released along the coordinate of separation of the PES) will be inefficiently channeled into vibration. For **L+HH** the attacking atom A approaches BC rapidly up to the normal bonding separation before the repulsion is released (dynamics in which the interatomic distance $r_{AB}$ decreases to its equilibrium separation $r^0_{AB}$, and only then does $r_{BC}$ increase, which corresponds on the PES to a rectilinear path). Since the repulsion operates on an already existent A–B bond, vibrational excitation is indeed inefficient. This behavior was sufficiently atypical to be described as the "light-atom anomaly" (*53*).

For the more general case of a heavier attacking atom relative to the molecule under attack, the new bond is still extended ($r_{AB} > r^0_{AB}$) at the time that the bulk of the repulsion is released; we can symbolize this as A- -B ▪ C. In this case repulsion between the separating atoms B and C results in recoil of B, rather than of AB as a whole, that is, it gives rise to efficient internal excitation of the new bond A–B.

Since the solution of the collinear equations of motion can be pictured in terms of the motion of a mass sliding across a suitably scaled and skewed representation of the PES, it is instructive to consider the characteristic path across the PES in the latter, more general case. The fact that $r_{AB}$ decreases at the same time as $r_{BC}$ increases (we term the energy released in this phase "mixed" or $\mathscr{M}$) means that the sliding mass, rather than following a rectilinear path, is cutting the corner of the PES. Therefore, instead of approaching the exit valley from its head, it approaches the valley from the side; consequently it oscillates from side to side of the exit valley, indicating that the new bond is vibrationally excited.

The proportion of the energy released during corner cutting is clearly relevant to the efficiency with which the repulsive energy is channeled into vibration. We have determined the extent of mixed energy release $\mathscr{M}_T$ from a specimen collinear trajectory that used the appropriate mass combination and the PES in question (*11, 53, 60*). Figure 8 shows that % $\mathscr{M}_T$ is insignificant for **L+HH**. For other mass combinations it is large.

If we turn to the experimental findings discussed above, the evidence favors strongly repulsive PESs, with the light-atom anomaly explaining both the markedly reduced $\langle f'_v \rangle$ for H + $X_2$ as compared with X + $H_2$ or X + HY, and the lower barrier leading to a slightly increased $\mathscr{A}_\perp$ in H + $Br_2$ as compared with H + $Cl_2$ (compare with the correlation noted above) accounting for the greater $\langle f'_v \rangle$ observed for H + $Br_2$ than for H + $Cl_2$ (*18*). Strongly repulsive PESs have successfully accounted for the general forms of the triangle plots (*61–64*). In the case of F + $H_2$ there is now dependable evidence from ab initio variational treatments of FHH (*65, 66*) that the energy release is indeed substantially repulsive.

The discussion of the previous paragraphs as it relates to repulsive energy release is summarized pictorially in Fig. 9. Actual tests of the validity of PESs are, of course, made by three-dimensional (3-D) trajectories. Product rotational excitation is eliminated from the picture in the collinear world. Although this is a minor constituent of the product energy, it is revealing of the dynamics. In the visualization of Fig. 9, we have included the effect of repulsive energy release in bent configurations as one source of product rotation. The experimental data in the triangle plots of Fig. 6 give persuasive evidence of the significance of this effect in the reaction F + $H_2$. Product repulsion would be expected (*44*) on the basis of momentum conservation to give rise to decreasing $\langle f'_R \rangle$ in the series FH▪D > FH▪H > FD▪D > FD▪H (the square indicates the locus of the repulsion); this is found theoretically, in 3-D trajectory studies, and also experimentally. The triangle plots of Fig. 6 correspond to the extremes of this range of isotopic mass combinations; $\langle f'_R \rangle$ for the FH▪D pathway substantially exceeds that for FH▪H.

Qualitative pictures of the type given in Fig. 9 suggest simple models of the reactive event (*59*). Despite their crudity, simple models have the important virtue that their "moving parts" are open to inspection.

The simple harmonic model (*60*) has been used to improve our understanding of the mechanism of mixed energy release, in which a repulsive force operating between particles B and C drives an oscillator joining A to B that is under tension. The model shows that for a wide range of conditions mixed energy release can play a significant role in channeling product repulsion into vibration.

The DIPR (direct interaction with product repulsion) model (*67*) sidesteps consideration of forces in the new bond by obtaining the product vibration $V'$ from $E'_{tot} - (R' + T')$, where $E'_{tot}$ is the product rotational excitation. From the direction of recoil of atom C relative to the direction of approach of A, angular distributions can readily be generated in three dimensions. The model provides a simple means to expose the link between the angular distribution of reaction products and their internal excitation, as well as the connection between these two quantities and the collision energy.

Findings for the DIPR model are summarized in Fig. 10 (solid lines). The interactions become less repulsive (more attractive) from left to right. This is achieved by systematically decreasing the repulsive impulse [the time integral of the force, $F(t)$, between B and C] which alone governs the dynamics. Since a measure of $\int F(t)\,dt$ can be obtained by a variety of means for any actual reactive PES (*59, 67*), the model can be tested by being applied to cases for which the results of 3-D trajectory computation are known. The agreement is excellent (see the points for the more repulsive cases in Fig. 10), so long as the assumption of direct interaction remains valid.

The lessons that can be learned from Fig. 10 are that strongly repulsive energy release will tend to give backward scattering of the molecular product ($\theta_{mol}$ is substantial at 180°) coupled with moderate internal excitation $E'_{int}$. As the repulsion is decreased, $\theta_{mol}$ shifts forward and $E'_{int}$ increases. The same effect can be achieved by increasing the reactant collision energy, since this too has the effect of decreasing the repulsive impulse $\int F(t)\,dt$.

Herschbach and co-workers have injected physical content into

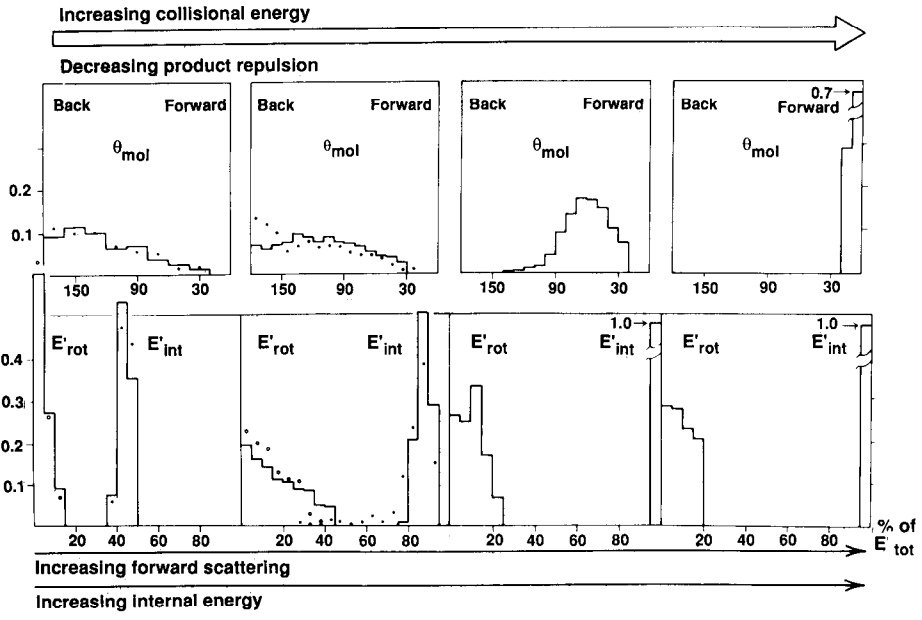


**Fig. 10.** Effect of repulsive energy release on product angular distribution (top row) and energy distribution (bottom row; $E'_{tot}$ is product rotational excitation and $E'_{int}$ is vibration plus rotation). The solid lines show the results of 3-D DIPR model calculations (masses K + $Br_2$, energy release $E'_{tot}$ = 53 kcal/mole). The total product repulsion used in the DIPR model calculations was decreased in four stages, from left to right in the figure, which simulated decreased % $\mathcal{R}$, and implied increased % $\mathcal{A}$. According to the DIPR model, this is mathematically equivalent to increasing the reagent collision energy, hence the dual label of the arrow at the top. The consequences of these changes are summarized qualitatively by the arrows at the foot of the figure. The dots record the distributions obtained from 3-D trajectories on potential-energy hypersurfaces with comparable partitioning of the energy release. [Courtesy of *The Journal of Chemical Physics* (*67*)]

the DIPR model in their DIPR–DIP extension, in which the repulsive impulse is assumed to be "distributed as in photodissociation" (*68*). The model then accounts nicely for product distributions observed in a number of reactions. More recently Zare and coworkers have shown how the DIPR approach can be used to understand the plane of rotation of newborn reaction products (*69*).

The FOTO (forced oscillation in a tightening oscillator) model (*70*), gives a fuller rendition of the forces on a collinear PES; the B•C repulsion operates on an AB oscillator whose force constant is increasing and whose equilibrium separation $r^0_{AB}$ is decreasing. The model, which has been applied to ten reactions for which experimental or theoretical data exist, is sufficiently complete to embody analogues of the "attractive," "mixed," and "repulsive" phases of energy release.

To the extent that the rotation in a newly formed reaction product AB originates in repulsion AB•C, the rotational motion should be coplanar with the repulsive force, and B in AB should recoil away from C (Fig. 11). This implies that the angle between the product rotational angular momentum vector **J**′ and the product orbital angular momentum vector **L**′ should be $\theta_{J'L'} \approx 180°$. Analyses of product distributions from 3-D trajectory studies (*64, 71*) bear this out. Experimental studies of correlations between such vector attributes will add materially to the mosaic from which our picture of reaction dynamics is composed.

The richer the detail in the rate constants $k(V',R',T')$, the clearer the message. The striking bimodality in the product energy distribution from H + ClI → HCl($v',J'$) + I recorded in Fig. 7 can be ascribed to "microscopic branching"; two patterns of molecular dynamics result in the formation of the same reaction product (HCl in this example). The dynamics have been explored in three dimensions for reasonable PESs (*51*). They are shown schematically in Fig. 12. In the case of H + ClI the migratory microscopic pathway (at the right of Fig. 12) is thought to dominate. This is for the same reason that macroscopic branching favors formation of HI rather than HCl, namely, the existence of a smaller energy barrier for approach from the I end of ICl [see (*72, 73*)] for the greater stability of ClIH than HClI. In collisions of H atoms with the I end of ICl that fail to yield HI, the H atom can migrate toward the Cl end of the molecule to yield highly internally excited HCl. The HCl product with low internal excitation comes from H atoms that have reacted directly at the Cl end of ClI. Since the barrier to this mode of reaction is higher, the yield (at normal reagent energies) is lower. It is evident that the relative yields of HCl and HI in macroscopic branching are linked to the yields of low $E'_{int}$ and high $E'_{int}$ HCl by way of microscopic branching.

Microscopic branching is thought to constitute more than merely an interesting curiosity, since it can contribute to the dynamics in any case where macroscopic branching is possible which encom-

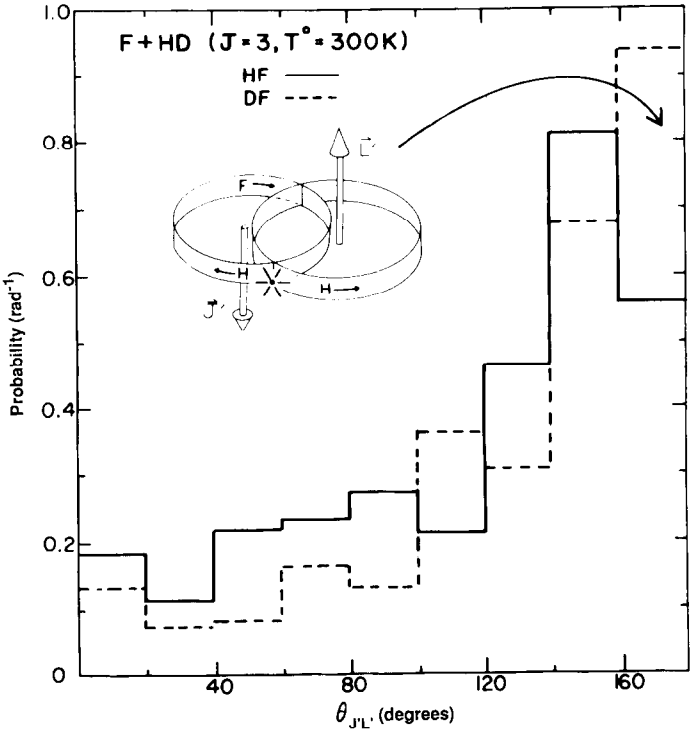


**Fig. 11.** Computed distribution $\theta_{J'L'}$ of the angle between the product rotational angular momentum **J**′ and orbital angular momentum **L**′ after repulsive energy release between the products of the reaction F + HD → HF + D (solid line) and F + HD → DF + H (broken line). At the extreme left $\theta_{J'L'} = 0°$ corresponds to **J**′ parallel to **L**′, while at the extreme right $\theta_{J'L'} = 180°$ corresponds to the favored outcome of **J**′ antiparallel to **L**′. [Courtesy of *The Journal of Chemical Physics* (*71*)]

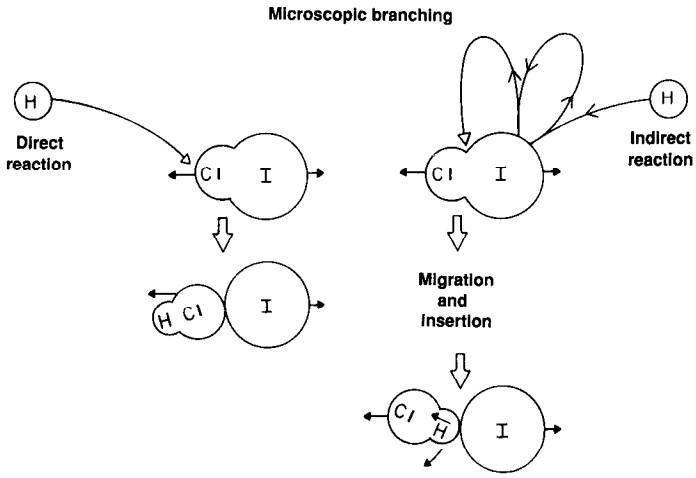


**Fig. 12.** Pictorial representation of the alternative dynamics, direct and indirect, in the microscopic branching underlying the bimodality of product energy distribution exemplified in Fig. 7. [Based on a classical trajectory study; see (*51*)]

passes a large class of reactions. As would be expected, the importance of microscopic branching, in common with macroscopic branching, is sensitive to the reagent energy (*38, 49, 50*).

## Channeling Reagent Energy into Products

*Experiment.* To increase the collision energy we formed atomic reagents [Cl for Cl + HI (*49*), F for F + HCl or F + $D_2$ (*50*), and H for H + $Cl_2$ (*50*)] by pyrolysis rather than using room temperature atoms. The effect is shown for H + $Cl_2$ in the triangle plot of Fig. 13. Comparison with the earlier 300 K triangle plot (Fig. 2) shows marked changes. The additional reagent translation $\Delta T$ in excess of the barrier to reaction has been channeled principally into additional product translation.

A second repository for this additional reagent energy was product rotation. The general finding regarding the disposition of additional reagent translation could be summarized as

$$\Delta T \rightarrow \Delta T' + \Delta R' \qquad (4)$$

This describes the average behavior.

By heating the molecular species under attack, or vibrationally exciting it in a prior reaction (*74*) and recording the change in product energy distribution (see, for example, Fig. 14), we found evidence of a similar adiabaticity, on the average, in regard to the conversion of reagent vibration into product excitation,

$$\Delta V \rightarrow \Delta V' \qquad (5)$$

(the symbol Δ denotes energy in excess of that required for barrier crossing).

*Theory.* The nature and the origins of the approximate adiabaticity relations (Eqs. 4 and 5) have been discussed in a number of places (*44, 49, 50, 54, 61, 75–78*). The origin of this adiabaticity is evident from an inspection of trajectories with and without the additional reagent energy. The effect of enhanced translation is to shift the characteristic pathway across the collinear PES (used as a diagnostic of 3-D behavior) toward more compressed configurations. The sliding mass impelled by its enhanced momentum along $r_{AB}$ caroms into the corner of the PES region 1 in Fig. 15. If the compressed intermediate A▪B▪C is collinear, it then flies apart to give translation in AB + C, and, if it is bent, to give enhanced rotation in

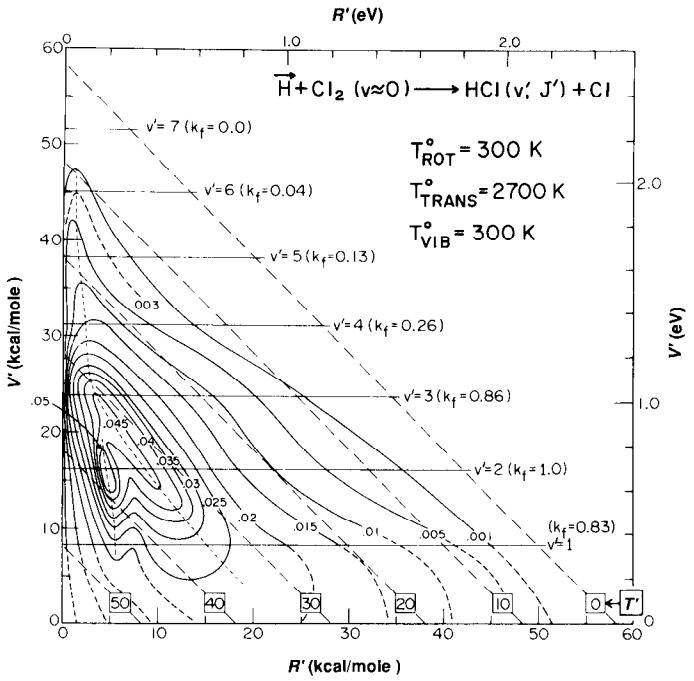


**Fig. 13.** Effect of enhanced reagent collision energy on the product energy distribution, that is, experimental values of $k(V',R',T')$ for H + $Cl_2(v = 0) \rightarrow HCl(v',J')$ + Cl. Mean collision energy $\langle T \rangle \approx 10.6$ kcal/mole. Compare $k(V',R',T')$ for room temperature reaction in Fig. 6. [Courtesy of *Faraday Discussions of the Chemical Society* (*50*)]

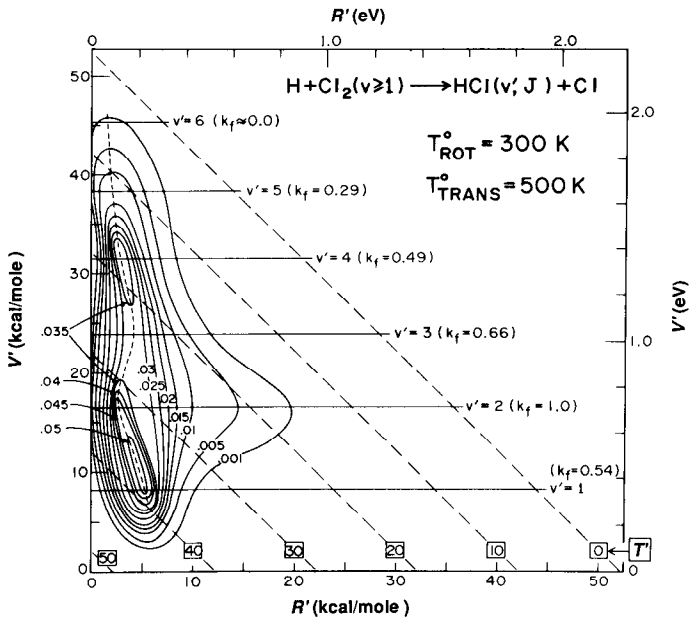


**Fig. 14.** Effect of enhanced reagent internal energy on the product energy distribution, that is, experimental $k(V',R',T')$ for H + $Cl_2(v \geq 1) \rightarrow HCl(v',J')$ + Cl. This result is approximate since it was obtained by subtracting the detailed rate constants for H + $Cl_2(v \approx 0) \rightarrow$ HCl + Cl from those for H + $Cl_2(v \geq 0) \rightarrow$ HCl + Cl. Mean vibrational energy $\langle V \rangle \approx 3.3$ kcal/mole. Compare with Fig. 2. [Courtesy of *Faraday Discussions of the Chemical Society* (*50*)]

AB. For enhanced reagent vibration the most common paths to product are shifted to region 2 in Fig. 15; the effect is to favor a more stretched intermediate A- - B- - C that pulls together along $r_{AB}$ to give AB($v >> 0$) + C. The opposite phase of vibration to that pictured in Fig. 15 drives the intermediate into region 1, giving rise to the low $V'$ peak in the product distribution.

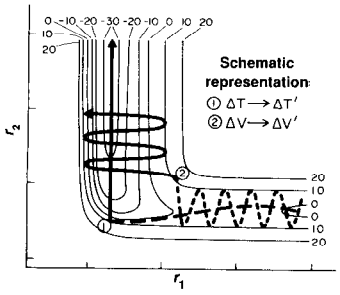


**Fig. 15.** Schematic representation (on a typical collinear exothermic PES) of the mechanism by which "additional" reagent translation ($\Delta T >> E_c$, where $E_c$ is the barrier height) is channeled into "additional" product translation ($\Delta T'$), and also of the mechanism 2, by which "additional" reagent vibration ($\Delta V >> E_c$) becomes "additional" product vibration ($\Delta V'$). (These are not actual trajectories, since they show neither the exothermic energy release nor the effect on that energy release of changing reagent energy; the intention, which is artificial, is to show the effect of $\Delta T$ and $\Delta V$ in isolation.) [Courtesy of *Faraday Discussions of the Chemical Society (50)*]

## Surmounting the Energy Barrier

*Experiment.* The most detailed information regarding the relative efficiency of various types of reagent motions in surmounting an energy barrier comes from the application of microscopic reversibility to detailed rate constants for the forward reaction $k_f(V',R',T')$ (*79*). Detailed rate constants for the reverse reaction $k_r(V',R',T')$ obtained in this way are recorded in the triangle plot of Fig. 16, where $V',R',T'$ are now the vibrational, rotational, and translational energies of the reagents for the endothermic reaction $HF(v',J') + H \rightarrow F + H_2$ (*80*). The total energy available for distribution is fixed by the nature of the experiment and is equal to the energy made available by the forward exothermic reaction (34.7 kcal/mole in the case illustrated). [This approach has been tested numerically by applying it to a case where $k_r(V',R',T')$ could be obtained directly from 3-D trajectories (*81*)]. Inspection of Fig. 16 indicates that a redistribution of 30 kcal/mole from $T'$ into $V'$ has the dramatic effect of increasing by a factor of $\sim 10^3$ the rate of reaction in the endothermic direction (*58, 80*).

In a few cases in other laboratories direct measurement has been made of the relative efficiency of vibration and translation in surmounting an energy barrier (*82–84*); in one of these cases (*84*) the barrier corresponded to a "substantially" (*44*) endothermic reaction; the reaction was $HF(v') + K \rightarrow H + KF$ (17 kcal/mole endothermic) and the effect of transferring 11 kcal/mole from reagent translation to vibration was to increase the reaction rate by a factor greater than 100.

The IR "chemiluminescence depletion" (CD) method, in which a prior reaction was used as a source of highly vibrationally excited reagent, was also used to obtain a measure of the efficiency of vibrational excitation in promoting endothermic reaction. Vibrational excitation was found to be highly efficient in carrying these reactions over their endothermic energy barriers (*85, 86*).

The CD approach was also used to map out the dependence of reaction rate on reagent rotational excitation (*87*). There was an initial decline in reaction probability with increasing $J$, followed by a rise. Similar behavior has been noted in crossed-beam experiments (*88, 89*).

*Theory.* We have found it revealing to link the preferred type of reagent energy distribution to the location of the energy barrier on the collinear PES. Figure 17 shows the dynamics characteristic of equal masses reacting across a PES with "early barrier" (surface I) and "late barrier" (surface II) (*90*). The effect of modest displacements of the barrier crest on the preferred mode of motion in the reagents was dramatic. On surface I a reagent translational energy only slightly in excess of the barrier height of 7 kcal/mole gave a calculable cross section, whereas a reagent vibrational energy double the barrier height gave a reactive cross section too small to be computed in our study. The converse behavior was found to apply on surface II.

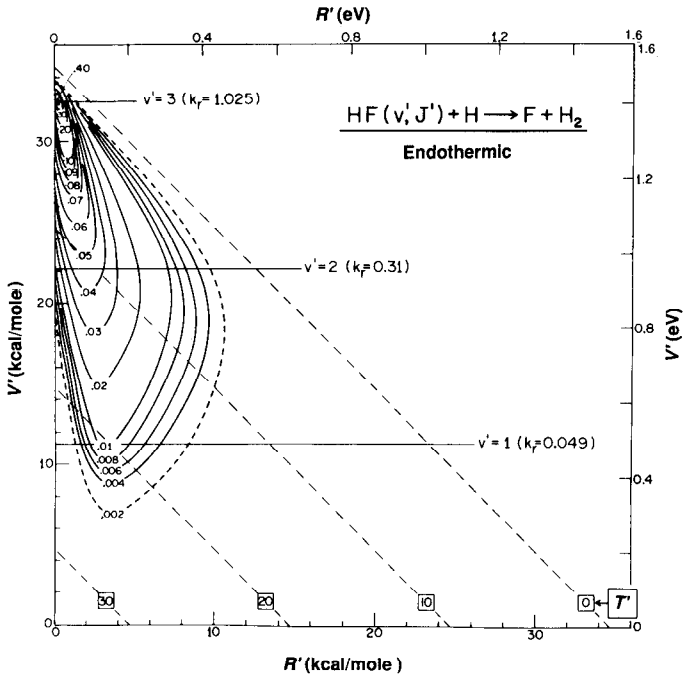


**Fig. 16.** Contours representing values of reagent vibrational, rotational, and translational energies for the endothermic reaction $HF(v',J') + H \rightarrow F + H_2$ which correspond to equal $k_r(\equiv k_{endo})$. The data were obtained by application of microscopic reversibility to the $k_f(\equiv k_{exo})$ given in Fig. 3. [Courtesy of *The Journal of Chemical Physics (80)*]

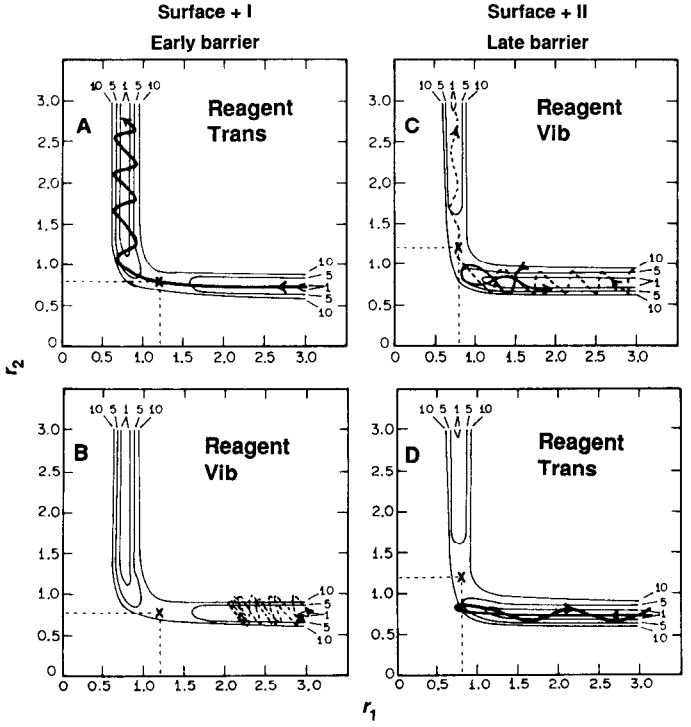


**Fig. 17.** (**A**) and (**B**) show specimen trajectories with (A) largely reagent translation ($T = 9$, $V = 0$) and (B) largely reagent vibration ($T = 1.5$ and $V = 14.5$) on an "early barrier" surface, that is, type I. (**C**) and (**D**) show trajectories with (C) largely reagent vibration ($T = 1.5$ and $V = 7.5$) and (D) largely reagent translation ($T = 16.0$, $V = 0$). All energies are in kilocalories per mole; reagent vibration is relative to $E(v = 0)$; the particles A, B, and C have equal mass. Positive and negative vibrational phases are shown with solid and broken lines, respectively. Barrier heights on both surfaces I and II are 7 kcal/mole; contours are labeled in kilocalories per mole. [Courtesy of *The Journal of Chemical Physics (90)*]

The correlations reduce to the proposition that a barrier predominantly along the coordinate of approach $r_{AB}$ is best traversed by motion in that same coordinate, namely, reagent translation, whereas a barrier predominantly along the coordinate of separation $r_{BC}$ is best traversed by motion in that coordinate, that is, vibration in the bond under attack. The trajectories in Fig. 17 (obtained by solution of the equations of motion, but capable of being pictured as the motion of a sliding mass across the PES) illustrate this; the reactive cases are (A) and (C) (early and late barriers) and the nonreactive cases are (B) and (D) (early and late barriers once again). The effect illustrated is sufficiently striking that it may also have relevance to the dynamics of reactions involving many atoms [see (*91*)], provided that these occur by a direct pathway.

The interest of these correlations is increased if we can link the form of the PES to the nature of the chemical reaction. Though unrecognized by reaction dynamicists, Hammond's postulate (*92*), namely, that for endothermic reactions the transition state resembles reaction products, might have pointed the way to the desired connection. Instead, a systematic study of a considerable number of exchange reactions A + BC → AB + C in terms of both the LEPS and the bond-energy bond-order (BEBO) methods led to the conclusion that for substantially exothermic reactions the barrier crest is located in the entrance valley (early barrier) of the PES, and for substantially endothermic reactions it is in the exit valley (late barrier) (*55*). From this, and the dynamical study of early and late barriers, it followed [as previously surmised (*93*)] that the favored degree of freedom for barrier crossing in substantially exothermic reactions would be translation, whereas reagent vibration would be most effective in giving rise to substantially endothermic reaction.

## Future Directions

Two further approaches could assist in the quest for understanding of the choreography of chemical reaction. In the first, attempts are being made to observe the molecular partners while they are, so to speak, on the stage, rather than immediately before and after the reactive dance. This is reactive "transition state spectroscopy" (TSS); it is a young but burgeoning field of experimentation [for theory, see (*94*); for experiment, see (*95*)]. In the second approach the intention, stated a little grandiosely, is to have a hand in writing the script according to which the dynamics occurs; this is "surface aligned photochemistry" (SAP), in which the reagents are aligned by the forces at a crystal surface and held in a fixed arrangement immediately prior to the initiation of the reaction by light, thus restricting the subsequent pattern of motion. Some success has been achieved experimentally. In addition a trajectory study (*96*) has shown the simplified link between product attributes and reactive geometries that applies under the more disciplined conditions of restricted angle of approach and impact parameter characteristic of SAP.

Even in the world of molecules the civilizing influence of modest restraints is a cause for rejoicing.

### REFERENCES AND NOTES


1. M. Beutler and M. Polanyi, *Z. Phys. Chem. B* **1**, 3 (1928); St. v. Bogdandy and M. Polanyi, *ibid.* **1**, 21 (1928); M. Polanyi and G. Schay, *ibid.*, p. 30.
2. D. R. Bates and M. Nicolet, *J. Geophys. Res.* **55**, 301 (1950).
3. G. Herzberg, *J. R. Astron. Soc. Can.* **45**, 100 (1951).
4. J. D. McKinley, D. Garvin, M. Boudart, *J. Chem. Phys.* **23**, 784 (1955); T. M. Cawthorn and J. D. McKinley, *ibid.* **25**, 583 (1956).
5. F. J. Lipscomb *et al.*, *Proc. R. Soc. London Ser. A* **233**, 455 (1956).
6. J. K. Cashion and J. C. Polanyi, *J. Chem. Phys.* **29**, 455 (1958).
7. ———, *ibid.* **30**, 1097 (1959); *Proc. R. Soc. London Ser. A* **258**, 529 (1960); *ibid.*, p. 564; *ibid.*, p. 570.
8. A. L. Schawlow and C. H. Townes, *Phys. Rev.* **112**, 1940 (1958); A. M. Prokhorov, *Zh. Eksp. Teor. Fiz.* **34**, 1658 (1958); *Sov. Phys. JETP* **7**, 1140 (1958).
9. J. C. Polanyi, *Proc. R. Soc. Can.* **54(C)**, 25 (1960).
10. ———, *J. Chem. Phys.* **34**, 347 (1961).
11. ———, *Appl. Op. Suppl.* **2**, 109 (1965).
12. C. K. N. Patel, W. L. Faust, R. A. McFarlane, *Bull. Am. Phys. Soc.* **119**, 500 (1964); C. K. N. Patel and R. J. Kerl, *Appl. Phys. Lett.* **5**, 81 (1964); C. K. N. Patel, *Phys. Rev. Lett.* **12**, 588 (1964).
13. J. V. V. Kasper and G. C. Pimentel, *Phys. Rev. Lett.* **14**, 352 (1965); G. C. Pimentel, *Sci. Am.* **214**, 32 (April 1966).
14. P. E. Charters and J. C. Polanyi, *Discuss. Faraday Soc.* **33**, 107 (1962).
15. H. O. Pritchard, *ibid.*, p. 278.
16. J. C. Polanyi, *ibid.*, p. 279.
17. The film "Concepts in Reaction Dynamics" [prepared in collaboration with C. A. Parr and P. E. Charters (1970)] comes in 30- and 40-minute versions; it illustrates, with commentary, many of the types of dynamics discussed in this lecture. Copies of the film have been deposited in a number of countries. Inquiries should be made to the author at the University of Toronto.
18. K. G. Anlauf, P. J. Kuntz, D. H. Maylotte, P. D. Pacey, J. C. Polanyi, *Discuss. Faraday Soc.* **44**, 183 (1967).
19. P. D. Pacey and J. C. Polanyi, *J. Appl. Opt.* **10**, 1725 (1971).
20. D. H. Maylotte, J. C. Polanyi, K. B. Woodall, *J. Chem. Phys.* **57**, 1547 (1972).
21. K. G. Anlauf *et al.*, *ibid.*, p. 1561.
22. J. C. Polanyi and K. B. Woodall, *ibid.*, p. 1574.
23. J. C. Polanyi and J. J. Sloan, *ibid.*, p. 4988.
24. F. London, *Problem der Modernen Physik* (Sommerfeld Festschrift 1928), p. 104; *Z. Elektrochem.* **35**, 552 (1924).
25. H. Eyring and M. Polanyi, *Z. Phys. Chem. B* **12**, 279 (1931).
26. J. O. Hirschfelder and E. Wigner, *J. Chem. Phys.* **7**, 616 (1929).
27. F. T. Wall, L. A. Hiller, J. Mazur, *ibid.* **29**, 255 (1958); *ibid.* **35**, 1284 (1961).
28. N. C. Blais and D. L. Bunker, *ibid.* **37**, 2713 (1962); *ibid.* **39**, 315 (1962).
29. J. C. Polanyi, in *Transfert d'Energie dans les Gaz*, R. Stoops, Ed. (Interscience, New York, 1962), pp. 177–182, 526–528; J. C. Polanyi and S. D. Rosner, *J. Chem. Phys.* **38**, 1028 (1963).
30. M. G. Evans and M. Polanyi, *Trans. Faraday Soc.* **35**, 178 (1939).
31. For a review, see B. S. Agrawala and D. W. Setser, in *Gas Phase Chemiluminescence and Chemi-ionization*, A. Fontijn, Ed. (Elsevier, New York, 1985), p. 157.
32. B. M. Berquist *et al.*, *J. Chem. Phys.* **76**, 2972 (1982); B. M. Berquist, L. S. Dzelzkalns, F. Kaufman, *ibid.*, p. 2984; L. S. Dzelzkalns and F. Kaufman, *ibid.* **77**, 3508 (1982); *ibid.* **79**, 3836 (1983).
33. J. C. Weisshaar, T. S. Zwier, S. R. Leone, *ibid.* **75**, 4873 (1981); for a review, see C. E. Hamilton and S. R. Leone, in *Gas Phase Chemiluminescence and Chemi-ionization*, A. Fontijn, Ed. (Elsevier, New York, 1985), p. 139.
34. H. L. Welsh, C. Cumming, E. J. Stansbury, *J. Opt. Soc. Am.* **41**, 712 (1951); H. L. Welsh, E. J. Stansbury, J. Romanko, T. Feldman, *ibid.* **45**, 338 (1955).
35. N. Jonathan, C. M. Melliar-Smith, D. H. Slater, *Mol. Phys.* **20**, 93 (1971); N. Jonathan *et al.*, *ibid.* **22**, 561 (1971).
36. H. W. Chang and D. W. Setser, *J. Chem. Phys.* **58**, 2298 (1973); D. J. Bogan and D. W. Setser, *ibid.* **64**, 586 (1976).
37. J. C. Moehlmann and J. D. McDonald, *ibid.* **62**, 3061 (1975).
38. J. W. Hudgens and J. D. McDonald, *ibid.* **67**, 3401 (1977).
39. P. M. Aker, D. J. Donaldson, J. J. Sloan, *J. Phys. Chem.* **40**, 3110 (1986).
40. D. Brandt, L. W. Dickson, L. N. Y. Kwan, J. C. Polanyi, *Chem. Phys.* **39**, 189 (1979); L. W. Dickson, thesis, University of Toronto (1982).
41. J. H. Parker and G. C. Pimentel, *J. Chem. Phys.* **51**, 91 (1969); R. D. Coombe and G. C. Pimentel, *ibid.* **59**, 251 (1973); *ibid.*, p. 1535; M. J. Berry, *ibid.*, p. 6229.
42. D. M. Neumark, A. M. Wodtke, G. N. Robinson, C. C. Hayden, Y. T. Lee, *ibid.* **82**, 3045 (1985); D. M. Neumark *et al.*, *ibid.*, p. 3067.
43. R. B. Bernstein and R. D. Levine, *ibid.* **57**, 434 (1972); *Advances in Atomic and Molecular Physics* (Academic Press, New York, 1975), vol. 11; R. B. Bernstein and R. D. Levine, in *Modern Theoretical Chemistry*, vol. 3B of *Dynamics of Molecular Collisions*, W. H. Miller, Ed. (Plenum, New York, 1976), chap. 7.
44. D. S. Perry and J. C. Polanyi, *Chem. Phys.* **12**, 419 (1976).
45. K. G. Anlauf *et al.*, *J. Chem. Phys.* **53**, 4091 (1970).
46. H. Heydtmann and J. C. Polanyi, *J. Appl. Opt.* **10**, 1738 (1971).
47. M. A. Nazar, J. C. Polanyi, W. J. Skrlac, *Chem. Phys. Lett.* **29**, 473 (1974); J. C. Polanyi and W. J. Skrlac, *Chem. Phys.* **23**, 167 (1977).
48. D. Brandt and J. C. Polanyi, *ibid.* **35**, 23 (1978); *ibid.* **45**, 65 (1980).
49. L. T. Cowley, D. S. Horne, J. C. Polanyi, *Chem. Phys. Lett.* **12**, 144 (1971).
50. A. M. G. Ding, L. J. Kirsch, D. S. Perry, J. C. Polanyi, J. L. Schreiber, *Faraday Discuss. Chem. Soc.* **55**, 252 (1973).
51. J. C. Polanyi, J. L. Schreiber, W. J. Skrlac, *ibid.* **67**, 66 (1979).
52. J. C. Polanyi, *J. Quant. Spectros. Radiat. Transfer* **3**, 471 (1963).
53. P. J. Kuntz *et al.*, *J. Chem. Phys.* **44**, 1168 (1966).
54. D. S. Perry, J. C. Polanyi, C. Woodrow Wilson, Jr., *Chem. Phys.* **3**, 317 (1974).
55. M. H. Mok and J. C. Polanyi, *J. Chem. Phys.* **51**, 1451 (1969).
56. T. H. Dunning, Jr., *J. Phys. Chem.* **88**, 2469 (1984).
57. J. C. Polanyi, *Discuss. Faraday Soc.* **44**, 293 (1967).
58. For a review, see J. C. Polanyi, *Acc. Chem. Res.* **5**, 161 (1972).
59. For a review, see J. C. Polanyi and J. L. Schreiber, in *Kinetics of Gas Reactions*, vol. 6A of *Physical Chemistry—An Advanced Treatise*, H. Eyring, W. Jost, D. Henderson, Eds. (Academic Press, New York, 1974), p. 383.
60. P. J. Kuntz, E. M. Nemeth, J. C. Polanyi, *J. Chem. Phys.* **50**, 4607 (1969).
61. C. A. Parr, J. C. Polanyi, W. H. Wong, *ibid.* **58**, 5 (1973).
62. J. T. Muckerman, *ibid.* **54**, 1155 (1971); *ibid.* **56**, 2997 (1972); *ibid.* **57**, 3388 (1972).
63. J. C. Polanyi and J. L. Schreiber, *Chem. Phys. Lett.* **29**, 319 (1974).
64. ———, *Faraday Discuss. Chem. Soc.* **62**, 267 (1977).
65. C. F. Bender *et al.*, *Science* **176**, 1412 (1972).
66. H. F. Schaefer III, *J. Phys. Chem.* **89**, 5336 (1985).
67. P. J. Kuntz, M. H. Mok, J. C. Polanyi, *J. Chem. Phys.* **50**, 4623 (1969).
68. D. R. Herschbach, *Faraday Discuss. Chem. Soc.* **55**, 233 (1973).
69. M. G. Prisant, C. T. Rettner, R. N. Zare, *J. Chem. Phys.* **81**, 2699 (1984).
70. M. D. Pattengill and J. C. Polanyi, *Chem. Phys.* **3**, 1 (1974).
71. N. H. Hijazi and J. C. Polanyi, *J. Chem. Phys.* **63**, 2249 (1975); *Chem. Phys.* **11**, 1 (1975).

72. A. D. Walsh, *J. Chem. Soc.* **1953**, 2266 (1953).
73. J. J. Valentini, M. J. Coggiola, Y. T. Lee, *J. Am. Chem. Soc.* **98**, 853 (1976); *Faraday Discuss. Chem. Soc.* **62**, 232 (1977).
74. B. A. Blackwell, J. C. Polanyi, J. J. Sloan, *Chem. Phys.* **24**, 25 (1977).
75. D. L. Thompson, *J. Chem. Phys.* **56**, 3570 (1972).
76. J. C. Polanyi, *Faraday Discuss. Chem. Soc.* **55**, 389 (1973).
77. ———, J. L. Schreiber, J. J. Sloan, *Chem. Phys.* **9**, 403 (1975).
78. J. C. Polanyi, J. J. Sloan, J. Wanner, *ibid.* **13**, 1 (1976).
79. K. G. Anlauf, D. H. Maylotte, J. C. Polanyi, R. B. Bernstein, *J. Chem. Phys.* **51**, 5716 (1969).
80. J. C. Polanyi and D. C. Tardy, *ibid.*, p. 5717.
81. D. S. Perry, J. C. Polanyi, C. Woodrow Wilson, Jr., *Chem. Phys. Lett.* **24**, 484 (1974).
82. T. J. Odiorne, P. R Brooks, J. V. V. Kasper, *J. Chem. Phys.* **55**, 1980 (1971); J. G. Pruett, F. R. Grabiner, P. R Brooks, *ibid.* **63**, 3335 (1974); *ibid.*, p. 1173.
83. A. Gupta, D. S. Perry, R. N. Zare, *ibid.* **72**, 6237 (1980); *ibid.*, p. 6250.
84. F. Heismann and H. J. Loesch, *Chem. Phys.* **64**, 43 (1982).
85. D. J. Douglas, J. C. Polanyi, J. J. Sloan, *J. Chem. Phys.* **59**, 6679 (1973).
86. F. E. Bartoszek, B. A. Blackwell, J. C. Polanyi, J. J. Sloan, *ibid.* **74**, 3400 (1981).
87. B. A. Blackwell, J. C. Polanyi, J. J. Sloan, *Chem. Phys.* **30**, 299 (1978).
88. H. H. Dispert, M. W. Geis, P. R. Brooks, *J. Chem. Phys.* **70**, 5317 (1979).
89. M. Hoffmeister, L. Potthast, H. J. Loesch, *Book of Abstracts, Twelfth International Conference on the Physics of Electronic and Atomic Collisions* (Gatlinburg, 1981).
90. J. C. Polanyi and W. H. Wong, *J. Chem. Phys.* **51**, 1439 (1969).
91. M. H. Mok and J. C. Polanyi, *ibid.* **53**, 4588 (1970).
92. G. S. Hammond, *J. Am. Chem. Soc.* 77, 334 (1955).
93. J. C. Polanyi, *J. Chem. Phys.* **31**, 1338 (1959).
94. T. F. George, *J. Phys. Chem.* **86**, 10 (1982), and references therein; A. M. F. Lau, *Phys. Rev. A* **13**, 139 (1976); *ibid.* **14**, 279 (1976); *Phys. Rev. Lett.* **43**, 1009 (1978); *Phys. Rev. A* **22**, 614 (1980); V. S. Dubov, L. I. Gudzenko, L. V. Gurvich, S. I. Yakovlenko, *Chem. Phys. Lett.* **45**, 330 (1977); S. I. Yakovlenko, *Sov. J. Quantum Electron.* **8**, 151 (1977); A. E. Orel and W. H. Miller, *Chem. Phys. Lett.* **57**, 362 (1979); *J. Chem. Phys.* **70**, 4393 (1979); J. C. Light and A. Altenberger-Siczek, *ibid.*, p. 4108; J. C. Polanyi, *Faraday Discuss. Chem. Soc.* **67**, 129 (1979); ——— and R. J. Wolf, *J. Chem. Phys.* **75**, 5951 (1981); H. R. Mayne, R. A. Poirier, J. C. Polanyi, *ibid.* **80**, 4025 (1984); H. R. Mayne, J. C. Polanyi, N. Sathyamurthy, S. Raynor, *ibid.* **88**, 4064 (1984); V. Engel, Z. Bacic, R. Schinke, M. Shapiro, *ibid.* **82**, 4844 (1985); V. Engel and R. Schinke, *Chem. Phys. Lett.* **122**, 103 (1985); P. M. Agrawal, V. Mohan, N. Sathyamurthy, *ibid.* **114**, 343 (1985).
95. P. Arrowsmith *et al.*, *J. Chem. Phys.* **73**, 5895 (1980); H. J. Foth, J. C. Polanyi, H. H. Telle, *J. Phys. Chem.* **86**, 5027 (1982); P. Arrowsmith, S. H. P. Bly, P. E. Charters, J. C. Polanyi, *J. Chem. Phys.* **79**, 283 (1983); P. Hering, P. R. Brooks, R. F. Curl, Jr., R. S. Judson, R. S. Lowe, *Phys. Rev. Lett.* **44**, 657 (1980); P. R. Brooks, R. F. Curl, T. C. Maguire, *Ber. Bunsenges. Phys. Chem.* **86**, 401 (1982); H. P. Grieneisen, H. Xue-Jing, K. L. Kompa, *Chem. Phys. Lett.* **82**, 421 (1981); J. K. Ku, G. Inoue, D. W. Setser, *J. Phys. Chem.* **87**, 2989 (1983); T. C. Maguire, P. R. Brooks, R. F. Curl, J. H. Spence, S. Ulrick, *J. Chem. Phys.* **85**, 844 (1986); *Phys. Rev. A* **34**, 4418 (1986); P. D. Kleiber, A. M. Lyyra, K. M. Sando, S. P. Heneghan, W. C. Stwalley, *Phys. Rev. Lett.* **54**, 2003 (1985); P. D. Kleiber, A. M. Lyyra, K. M. Sando, V. Zafiropolos, W. C. Stwalley, *J. Chem. Phys.* **85**, 5493 (1986).
96. E. B. D. Bourdon *et al.*, *J. Phys. Chem.* **88**, 6100 (1984); E. B. D. Bourdon *et al.*, *Faraday Discuss. Chem Soc.* **82**, (1986).
97. The research described here insofar as it related to the work of this laboratory was performed over a 30-year period at the University of Toronto. It is a pleasure to express indebtedness to my colleagues at this university, most especially to the late D. J. LeRoy, who fostered this work from its inception, and to my students and postdoctoral associates whose talents, generosity, and friendship have made this undertaking possible and fulfilling.